Supplementary Information

A simple, low-cost CVD route to thin films of BiFeO$_3$ for efficient water photo-oxidation

Savio J. A. Moniz,[a,b] Raul Quesada-Cabrera,[a] Christopher S. Blackman,[a,*] Junwang Tang,[b] Paul Southern,[c] Paul M. Weaver[d] and Claire J. Carmalt.[a]

* Email: c.blackman@ucl.ac.uk
[a] *Materials Chemistry Centre, Department of Chemistry, University College London, 20 Gordon Street, London, WC1H 0AJ, United Kingdom.*
[b] *Department of Chemical Engineering, University College London, Torrington Place, London WC1E 7JE, United Kingdom.*
[c] *UCL Healthcare Biomagnetics Laboratories, 21 Albemarle Street, London, W1S 4BS, United Kingdom.*
[d] *National Physical Laboratory, Hampton Road, Teddington, Middlesex, TW11 0LW, United Kingdom.*

Experimental

Film Analysis: X-ray Diffraction was carried out using a Bruker-AXS D8 powder diffractometer equipped with a GADDS Hi-Star area detector, using Cu-K$_\alpha$ radiation (λ = 1.54056 Å) in the range 10 – 65° 2θ. Phase information was obtained from the Diffrac*plus* EVA program suite (Version 2) and ICSD. Scanning electron microscopy (SEM) was used in order to examine surface morphology and films thickness. Images were obtained on a Jeol JSM-6301F Field Emission Microscope at 5 kV, after coating samples with an ultrathin layer of gold to prevent charging. Quantitative analyses of bismuth and iron were carried out *via* WDX using a Philips XL30ESEM Machine operating at 10 kV, equipped with an Oxford Instruments INCA detector. Films were carbon coated prior to analysis to prevent charging. XPS analysis was performed using a Kratos AXIS Ultra machine with a delay line detector under a pressure of 10^{-9} torr. A monochromated Al-K$_\alpha$ X-ray source producing a full width at half maximum (FWHM) on the Ag 3d$_{5/2}$ peak of 0.48 eV was used. Raman spectra were acquired using a Renishaw Raman 1000 System using a helium-neon laser wavelength of 514.5 nm at room temperature (20 °C) and liquid nitrogen temperature (-195 °C) using a cold

stage and temperature controller equipped with a cryo pump. AFM analysis was performed using a Veeco Dimension 3100 machine in intermittent contact mode. UV-Vis spectra were recorded in transmission mode over the range 300 – 2500 nm using a Perkin Elmer Lambda 950 photospectrometer. Magnetism measurements (M-H hysteresis and ZFC-FC magnetisation) were conducted using a Quantum Design SQUID Vibrating Sample Magnetometer (VSM) with a maximum field setting of 7 T (70000 Oe). Films were mounted on a 4 mm diameter quartz rod using a vinyl phenolic adhesive (code GE7031, stable up to 400 K) and suspended parallel to the magnetic field (in-plane). Ferroelectric measurements (P-E hysteresis) were conducted at ambient temperature using aixPES tester from aixACCT systems set at an applied frequency of 1 kHz at an applied electric field of up to 125 kV cm^{-1}. $BiFeO_3$ films were grown directly onto 1 cm^2 $Pt/SiO_2/Si$ wafers; platinum top electrodes were deposited *via* sputtering using a 0.5 mm mask.

Photocatalytic oxygen evolution: Upon irradiation of the sample photo-generated holes produce oxygen molecules which can diffuse through the membrane and can subsequently be reduced at the Pt electrode according to Eq. (1). The Pt electrode is typically polarised at -0.6 V with respect to the silver electrode in order to carry out the reduction of oxygen. The oxidation-reduction takes place on the counter electrode with formation of AgCl, according to Eq. (2).

$$O_2 + 2H_2O + 4e^- \rightarrow 4OH^- \qquad \textbf{(Equation 1)}$$

$$4Ag + 4Cl^- - 4e^- \rightarrow 4AgCl \qquad \textbf{(Equation 2)}$$

The voltage recorded can be converted into moles of oxygen produced per time unit considering the amount of oxygen present in the air-saturated solution. The output of

the MPD cell is adjusted so that 1 V corresponds to air-saturated conditions whereas nitrogen saturation (i.e. the absence of oxygen) leads to a drop in the signal to 0 V. This voltage difference is given by the number of moles of oxygen dissolved in a certain volume of test solution, taking into account 21% of oxygen in air and a solubility of 40 mg dm^{-3} in water at 298 K. The output signal increases proportionally with respect to the rate of photo-generated oxygen produced.

The formal quantum efficiency (FQE) was calculated from the oxygen evolution rate as follows:

FQE = (Molecules formed (molecules cm^{-2} s^{-1}) / Photon Flux (photons cm^{-2} s^{-1}))*4 (4 electrons).

The O$_2$ yield (%) was therefore calculated as follows:

% O$_2$ yield = (Molecules formed (molecules cm^{-2} s^{-1}) / Photon Flux (photons cm^{-2} s^{-1})) * 4 (4 electrons) * 100 %

The light intensity (irradiance, W/cm^{-2}) of the UV lamp was measured using a calibrated UVX Radiometer. The photon flux was determined using:

Photon Flux (photons cm^{-2} s^{-1}) = Irradiance (W cm^{-2}) / Energy (J),

where Energy (J) = hc/λ, λ = 365 nm, h = Planck's constant, c = speed of light.

FIGURES
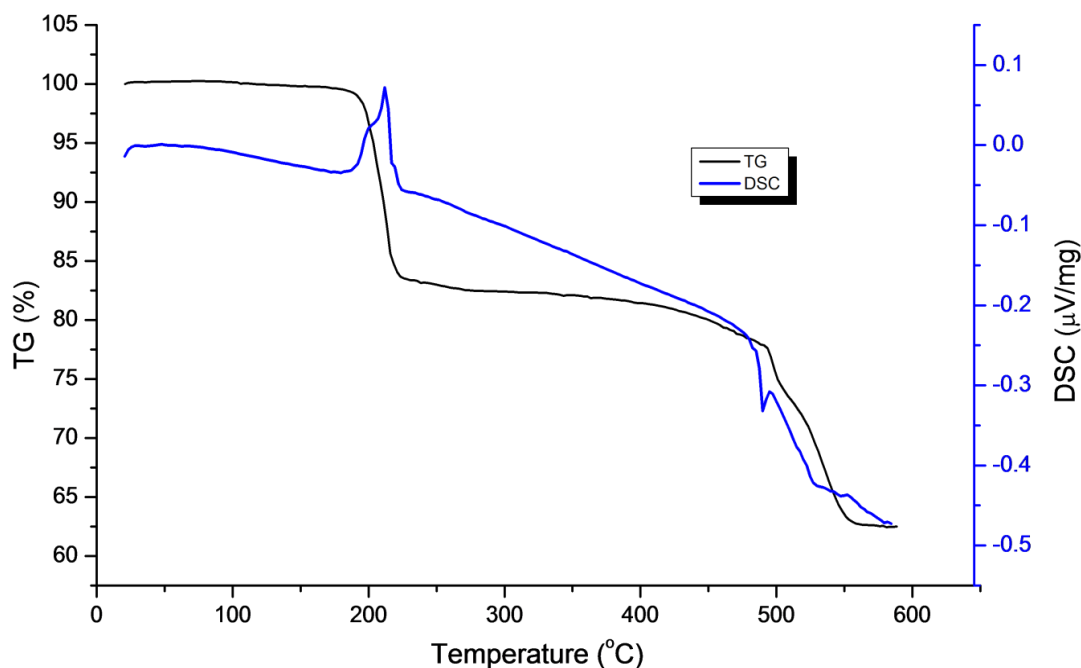
Figure 1: DSC-TGA pattern of [{Cp(CO)$_2$Fe}BiCl$_2$]

BiFeO$_3$ adopts a highly rhombohedrally distorted perovskite structure (polar space group $R3c$), with thirteen Raman active modes[1] – 4A$_1$ and 9E vibrations. Peaks that can be assigned to A$_1$ (147, 177, 223 and 475 cm^{-1}) and E (265, 282, 301, 354, 374, and 526 cm^{-1}) phonon modes were observed in the low temperature Raman spectra of a BiFeO$_3$ film obtained after annealing at 700 °C (Figure 2).[1,2] A peak observed at 550 cm^{-1} has previously been assigned to the TO forbidden vibrational mode of the fourth A$_1$ phonon vibration and observation of a broad peak around 1100 cm^{-1} suggests it is indeed associated with the 2TO mode.[3] Three broad peaks between 900 – 1400 cm^{-1} are similar to those observed by Ramirez *et al.*[4] for bulk and thin film BiFeO$_3$ samples.
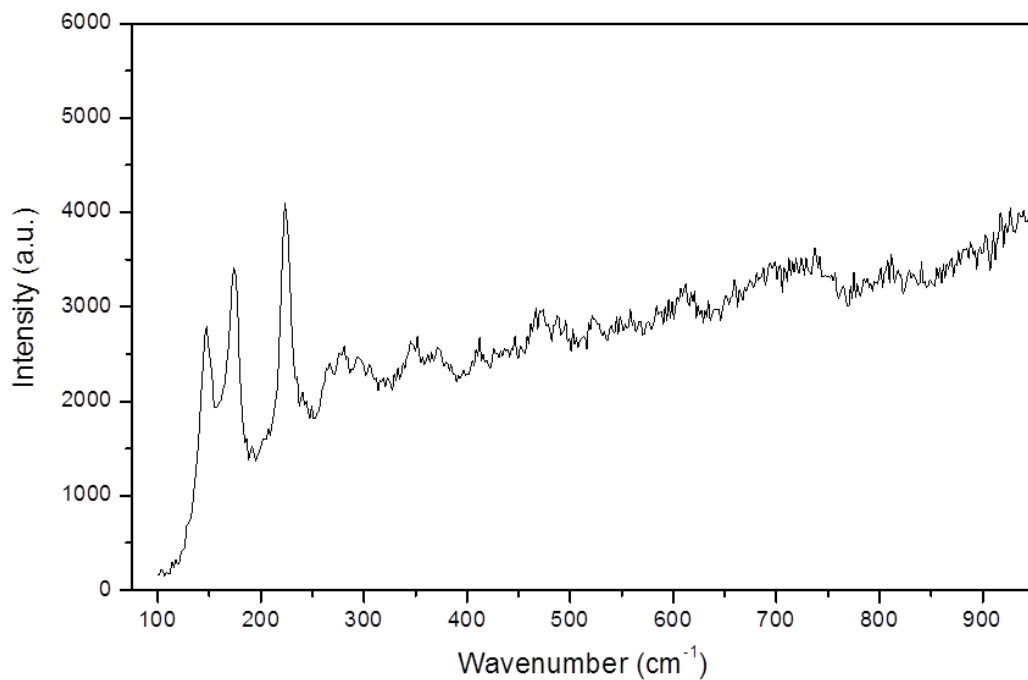
Figure 2: **Raman spectrum of the BiFeO$_3$ film formed after annealing at 700 °C, recorded at - 195 °C**
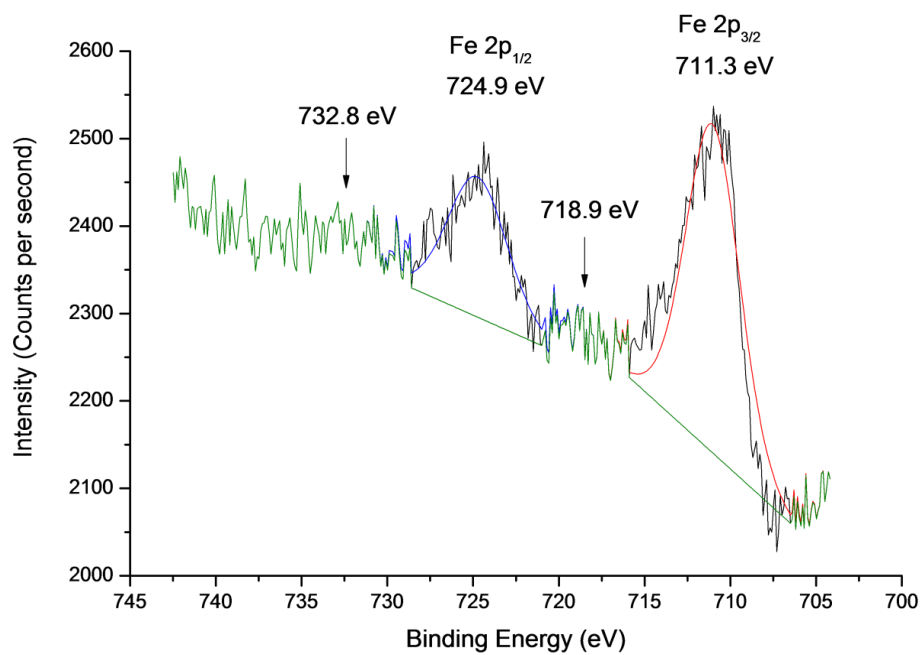

Figure 3: **XPS spectrum of the Fe 2p region of a BiFeO$_3$ thin film region after etching**
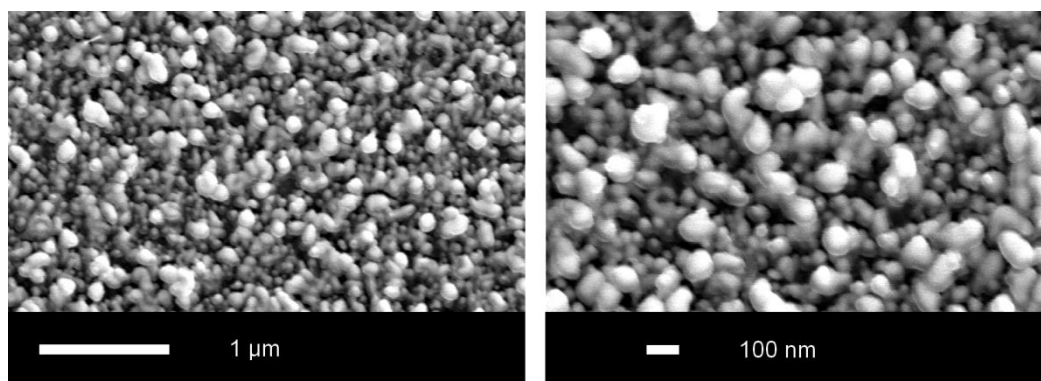
Figure 4: Top-down SEM images of Bi$_{24}$Fe$_2$O$_{39}$ film deposited on glass at 300 °C. Image on the left has 25,000x magnification, image on the right has 45,000x magnification.
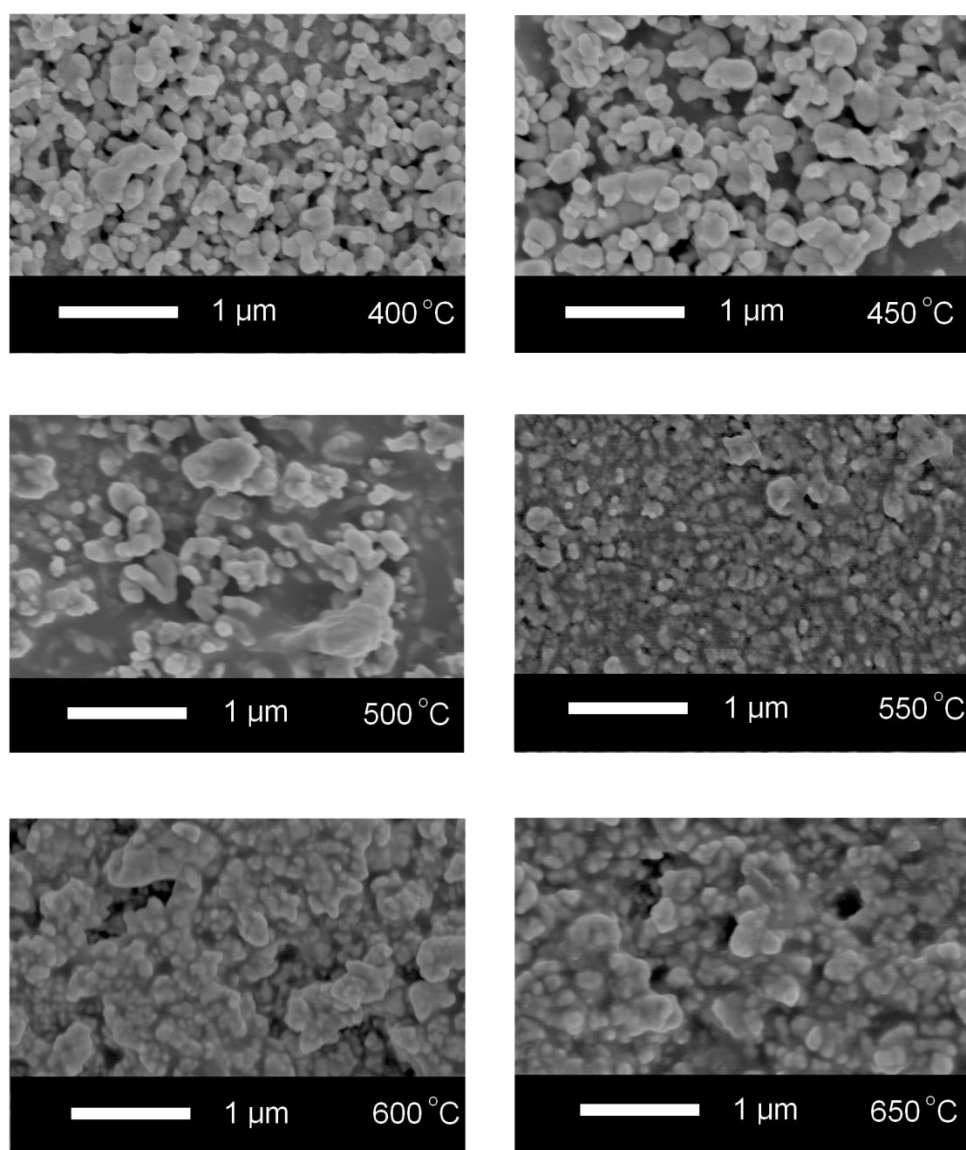

Figure 5: Top-down SEM images of the films annealed at the various temperatures specified within the diagram.

Films of $BiFeO_3$, grown by deposition directly onto 1 cm^2 Pt/SiO$_2$/Si wafers *via* AACVD followed by annealing at 700 °C, were investigated for their ferroelectric polarisation (Figure 6). The loop displays a polarisation peak at a lower field than the maximum, indicative of a degree of resistive behaviour and conduction through the material. This is common in bismuth ferrite systems[5] and has been reported in sol-gel[6] and PLD[7] films. These conductive contributions to the apparent polarisation mean that values obtained from such loops must be treated with caution.[8,9] A maximum polarisation of 8.7 µC/cm^2 was observed, providing an effective relative permittivity of almost 800. This high permittivity and non-linearity in the response is indicative of a strongly polar material, but is lower than reported for bulk ceramics[10] although the total polarisation is similar. The maximum polarisation is smaller than that for single crystal or epitaxial film bismuth ferrite (around 50 µC/cm^2),[11] but higher than those obtained for $BiFeO_3$ films grown *via* sol-gel processing (P_r = 1.8 µC/cm^2)[6] or PLD (P_r = 0.83 µC/cm^2),[7]. There could be a number of reasons for this such as domain pinning at defects preventing complete reversal of the polarisation and variation in orientation of the polar axis between crystallites. The high losses at this frequency mean that the polarisation at zero electric field from these loops cannot be accurately ascribed to the electrical remanence.
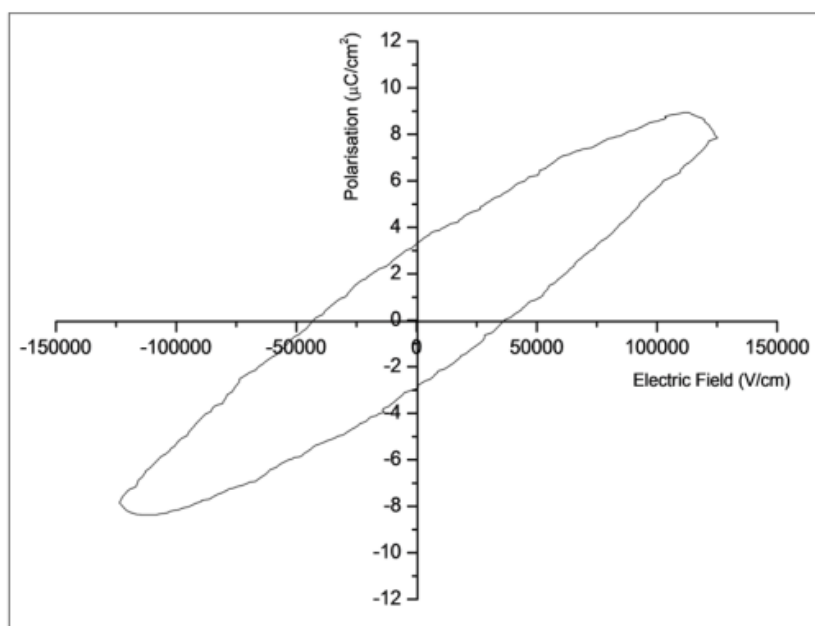
Figure 6: Room temperature P-E hysteresis loop measured at 1 kHz for a 300 nm thick BiFeO$_3$ film grown *via* AACVD and deposited on Pt/SiO$_2$/Si substrate sputtered with Pt top electrodes.

The temperature dependence of the magnetisation for a BiFeO$_3$ film displaying the field cooled (FC) and zero field cooled (ZFC) curves are shown in Figure 7 (b). The broad peak or "cusp" shown between 40 – 48 K in the ZFC data has been observed for larger particles (95 nm and above) of pure BiFeO$_3$[12] and is likely to correspond to the blocking temperature (or freezing temperature (T$_f$)) of the individual spins; the particle size in these films was estimated to be 110 nm (Scherrer equation), hence the appearance of this peak in the ZFC data. Another shift in the data seen at 132 K has not been observed previously in ZFC measurements however a spin-reorientation transition at ~ 140 K has been observed by Raman spectroscopy.[13] There is some deviation between the curves below 300 K and this is characteristic of spin-glass behaviour.[14] The dramatic increase in magnetisation below ~20 K is in agreement with the M-H curve (Figure 7 (a)) and suggests ferromagnetic behaviour. The large reduction in coercivity between the experiments run at 5 K and 300 K suggest low temperature superparamagnetic behaviour, in agreement with results from other groups.[15,14,16]
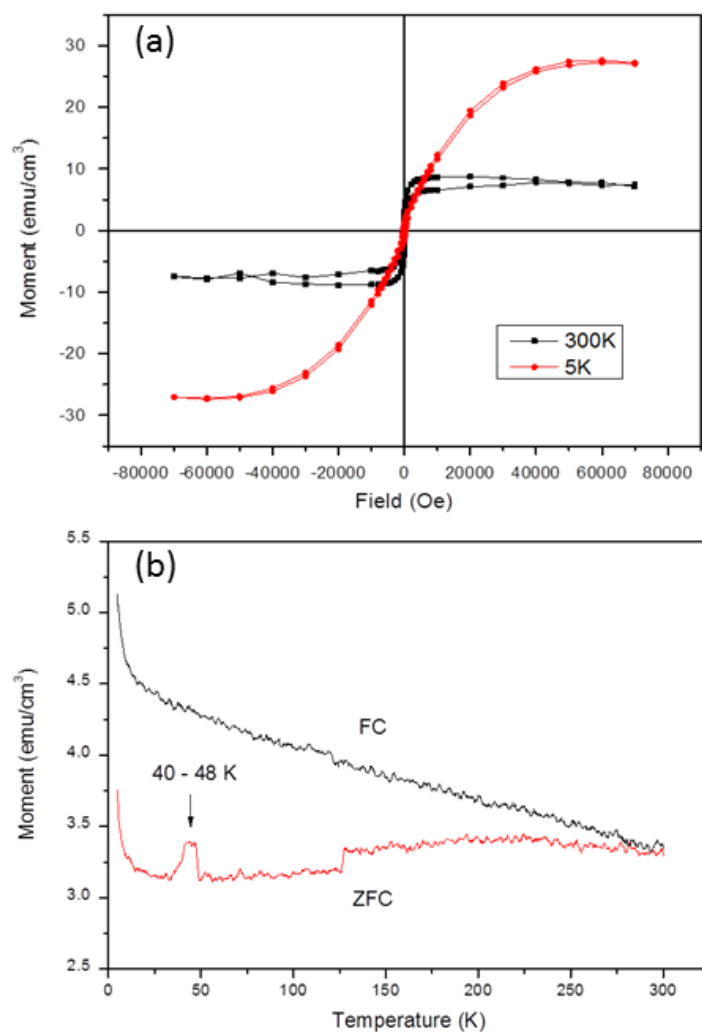
Figure 7: (a) M-H hysteresis loop measured at 5 K and (b) ZFC and FC curves measured at an applied field of 200 Oe for the 320 nm thick $BiFeO_3$ film prepared *via* AACVD and annealed at 700 °C.
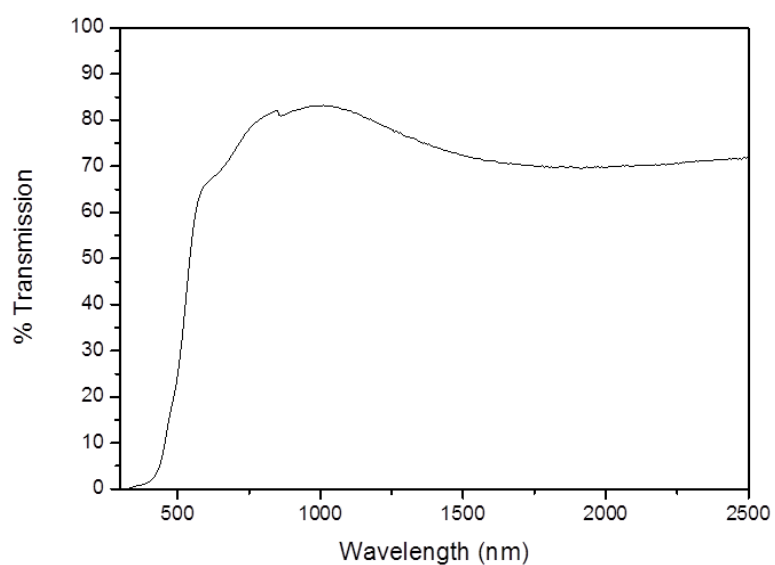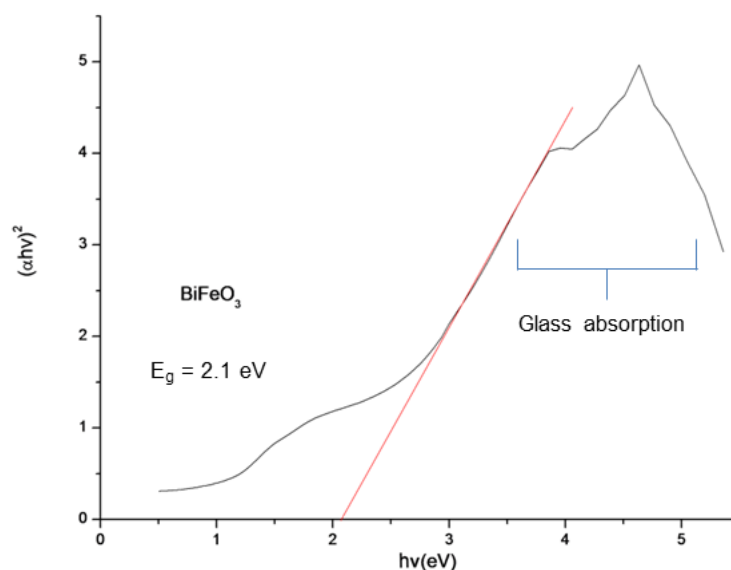

Figure 8: UV-Vis spectra of a pure $BiFeO_3$ film on a Corning glass substrate

Figure 9: **Tauc plot for a BiFeO$_3$ film formed *via* AACVD. The region between 4 – 5 eV is indicative of the absorption effects of the glass substrate at UV wavelengths.**

References

1. H. Fukumura, H. Harima, K. Kisoda, M. Tamada, Y. Noguchi, and M. Miyayama, *Journal of Magnetism and Magnetic Materials*, 2007, **310**, e367–e369.

2. D. Rout, K.-S. Moon, and S.-J. L. Kang, *Journal of Raman Spectroscopy*, 2009, **40**, 618–626.

3. M. Cazayous, D. Malka, D. Lebeugle, and D. Colson, *Applied Physics Letters*, 2007, **91**, 071910.

4. M. O. Ramirez, M. Krishnamurthi, S. Denev, A. Kumar, S.-Y. Yang, Y.-H. Chu, E. Saiz, J. Seidel, A. P. Pyatakov, A. Bush, D. Viehland, J. Orenstein, R. Ramesh, and V. Gopalan, *Applied Physics Letters*, 2008, **92**, 022511.

5. M. A. Khan, T. P. Comyn, and A. J. Bell, *Applied Physics Letters*, 2008, **92**, 072908.

6. Y. Wang, Q. Jiang, H. He, and C.-W. Nan, *Applied Physics Letters*, 2006, **88**, 142503.

7. V. R. Palkar, J. John, and R. Pinto, *Applied Physics Letters*, 2002, **80**, 1628.

8. M. Stewart, M. G. Cain, and D. Hall, *NPL Report CMMT(A)152*, 1999, 1–57.

9. W. Eerenstein, F. D. Morrison, S. F., J. L. Prieto, J. P. Attfield, J. F. Scott, and N. D. Mathur, *Philosophical Magazine Letters*, 2007, **87**, 249–257.

10. L. Curecheriu, F. Gheorghiu, A. Ianculescu, and L. Mitoseriu, *Applied Physics Letters*, 2011, **99**, 172904.

11. G. Catalan and J. F. Scott, *Advanced Materials*, 2009, **21**, 2463–2485.

12. T.-J. Park, G. C. Papaefthymiou, A. J. Viescas, A. R. Moodenbaugh, and S. S. Wong, *Nano Letters*, 2007, **7**, 766–772.

13. M. K. Singh, R. S. Katiyar, and J. F. Scott, *Journal of Physics: Condensed Matter*, 2008, **20**, 252203.

14. M. Singh, W. Prellier, M. Singh, R. Katiyar, and J. Scott, *Physical Review B*, 2008, **77**, 1–5.

15. F. Gao, Y. Yuan, K. F. Wang, X. Y. Chen, F. Chen, J.-M. Liu, and Z. F. Ren, *Applied Physics Letters*, 2006, **89**, 102506.

16. M. K. Singh, R. S. Katiyar, W. Prellier, and J. F. Scott, *Journal of Physics: Condensed Matter*, 2009, **21**, 042202.